Marine Science Center-University of Basrah

Mesopotamian Journal of Marine Sciences
Print ISSN: 2073-6428
E- ISSN: 2708-6097
www.mjms.uobasrah.edu.iq/index.php/mms

Landsat 8 Thermal Band Precision Assessment in Measuring the Arabian Gulf's Northwest Sea Surface Temperature

iD Adel J. Al-Fartusi [*1], Mutasim I. Malik[2] , iD Hameed M. Abduljabbar[3]
1- Physics Department, Marine Science Center, Basrah University, Basra - Iraq
2- Physics Department, Science College, Wasit University, Wasit- Iraq
3- Physics Department, College of Education for Pure Science, Ibn-Al-Haitham, Baghdad – Iraq
Corresponding Author: *e-mail: adel.mohammed@uobasrah.edu.iq*

Article info.
✓ *Received: 22 March 2026*
✓ *Accepted: 26 April 2026*
✓ *Published: 29 June2026*

Key Words:
Landsat 8
North West Arabian Gulf
SST
Thermal Band

Abstract - One of the most significant fields for remote sensing applications is physical oceanography research. Early methods for thermal mapping of the seas and oceans included using sensors mounted on buoys. Through the use of thermal sensors mounted on Earth observation satellites, remote sensing now offers more progressive techniques to extract the sea surface temperature (SST) values as a continuous raster model for all water bodies. Landsat 8's TIRS sensor must have a thermal band so that the SST can be extracted with a 100 m2 spatial resolution. The precision of two thermal bands from Landsat 8 (bands 10 and 11) for SST appreciation in waters northwest of the Arabian Gulf was confirmed by the current study. Using thermal images and comparing them with the actual measured temperatures of selected stations taken in December 2014 and January 2022. This was accomplished using the "Brightness Temperature" function provided by ENVI 5.3 for determining the surface temperature. By accounting for root mean square error (RMSE) and mean absolute error rate (MAPE), Landsat 8's precision for SST monitoring in waters northwest of the Arabian Gulf was confirmed. The thermal band 10's accuracy was ±1.72 (1.79%), while the precision of thermal band 11 was ±2.37 (2.49%) in 2014, with a difference of ± 0.65 (0.7%). In 2022, it was found that the precision of thermal band 10 was ± 1.7 (2.37%), and the precision of thermal band 11 was ± 2.25 (3.13%), with a difference of ± 0.55 (0.76%).Wherefore, the outputs of the current study show that Landsat 8's thermal band 10 is more precise than thermal band 11 at measuring the sea surface temperature of water northwest of the Arabian Gulf.

تقييم دقة النطاق الحراري لبيانات القمر الصناعي لاندسات 8 في قياس درجة حرارة سطح البحر – شمال غرب الخليج العربي

عادل جاسم الفرطوسي[1]، معتصم ابراهيم ملك[2] ، حميد مجيد عبد الجبار[3]
1- مركز علوم البحار ، جامعة البصرة ، البصرة – العراق
2- كلية العلوم، جامعة واسط، واسط – العراق
3- كلية التربية للعلوم الصرفة (ابن الهيثم) ، جامعة بغداد، بغداد - العراق

المستخلص – يُعدّ البحث في علم المحيطات الفيزيائي أحد أهم مجالات تطبيقات الاستشعار عن بُعد. تضمنت الطرق المبكرة لرسم الخرائط الحرارية للبحار والمحيطات استخدام أجهزة استشعار مثبتة على عوامات. بفضل استخدام أجهزة الاستشعار الحراري المثبتة على أقمار مراقبة الأرض، يُقدّم الاستشعار عن بُعد اليوم تقنيات أكثر تطورًا لاستخراج قيم درجة حرارة سطح البحر (SST) كنموذج نقطي متصل لجميع المسطحات المائية. يجب أن يحتوي مستشعر TIRS الخاص بلاندسات 8 على نطاق حراري لاستخراج درجة حرارة سطح البحر بدقة مكانية تبلغ 100 متر مربع. أكدت هذه الدراسة دقة نطاقين حراريين من لاندسات 8 (النطاقان 10 و11) في تقدير درجة حرارة سطح البحر في المياه الواقعة شمال غرب الخليج العربي. تم استخدام الصور الحرارية ومقارنتها بدرجات الحرارة المقاسة فعليًا في محطات مختارة خلال شهري كانون الاول 2014 وكانون الثاني 2022. وقد تم

DOI:https://doi.org/10.58629/mjms.v41i1.444 ,

ذلك باستخدام وظيفة "درجة حرارة السطوع" المتوفرة في برنامج ENVI 5.3 لتحديد درجة حرارة السطح. وباستخدام متوسط الجذر التربيعي للخطأ (RMSE) ومتوسط معدل الخطأ المطلق(MAPE) ، تم تأكيد دقة القمر الصناعي لاندسات 8 في رصد درجة حرارة سطح البحر في منطقة الدراسة. بلغت دقة النطاق الحراري 10 ± 1.72 (1.79%) ، بينما بلغت دقة النطاق الحراري 11 ± 2.37 (2.49%) في عام 2014، بفارق قدره ± 0.65 (0.7%). عام 2022 وُجد أن دقة النطاق الحراري 10 بلغت ± 1.7 (2.37%)، بينما بلغت دقة النطاق الحراري 11 ± 2.25 (3.13%)، بفارق قدره ± 0.55 (0.76%) .وبناءً على ذلك، تُظهر نتائج هذه الدراسة أن النطاق الحراري 10 في القمر الصناعي لاندسات 8 أكثر دقة من النطاق الحراري 11 في قياس درجة حرارة سطح البحر شمال غرب الخليج العربي.

الكلمات المفتاحية: لاندسات 8، النطاق الحراري، درجة حرارة سطح البحر، شمال غرب الخليج

Introduction:

A variety of ocean and atmospheric phenomena are observed and understood better with the help of sea surface temperature (SST). Accurate temperature measurement is obtained on-site, or it can be obtained by buoys or scientific research vessels. Additionally, sea surface temperatures tracked by satellites are important and have been successfully applied in practice (Corlett *et al.,* 2006 and Dash *et al.,* 2010). SST databases from satellite observations have been created, which were widely used for examining SST fronts (Ullman and Cornillon , 2000 ; Park *et al.,* 2004).

The biological diversity of marine life is affected by seawater temperature (SST), which is an important variable affecting the physical properties and in addition, is a good index of water quality (Wloczyk *et al.,* 2006). A small change in seawater temperature can have an impact on the environment, changing how marine creatures are distributed.

Furthermore, long-term SST mensuration is beneficial in climate research (Ahn *et al.,* 2006). Earlier on, studies have relied on extracting contour lines data from sensors mounted on buoys, then determining values from a crossing of the lines. This method is regarded for thermally mapping seas and oceans as one of the rudimental. A relatively recent study by (Elhakeem *et al.,* 2015), which concentrated on a long-term simulation of the Gulf's hydrodynamics, concluded that the warm water inflow from the Sea of Oman through the Strait of Hormuz, in addition to the meteorological effect, is the main factor regulating water evaporation during the winter (humidity, air temperature, cloud cover, and wind. (Xue and Eltahir, 2015) found that the annual surface evaporation in the Arabian Gulf is 1.84 m/year using a simulation model coupling between the atmosphere and the ocean, which agrees with (Reynolds, 1993). Having highlighted the important role that sea surface heat plays in heat transfer between water and the atmosphere by these studies.

Researching three-dimensional fields and computing derived quantities like heat fluxes are better suited for numerical modelling. However, remote sensing data is frequently the best for examining quantities at the sea surface, in part due to the avoidance of inaccurate numerical approximations of differential equations and complex physical process parameterizations. Additionally, remote sensing data can be used to verify numerical models (Nesterov *et al.,* 2021). Sea surface temperature measurements from space have been made possible since the 1980s thanks to Earth observation satellites (Syariz *et al.,* 2015).

One of the barriers to accurately measuring sea surface temperature has been the low spatial resolution. Therefore, to generate more accurate SST values, precise algorithms have been developed (Wloczyk *et al.,* 2006). Due to its inclusion of a Thermal Infrared Sensor (TIRS) with a spatial resolution of 100 m2, the free Landsat 8 satellite has marked a significant advancement in the field of thermal imaging. There are two bands for the TIRS sensor: (10.60 to 11.19 μm) for thermal infrared band 10, and (11.50 to 12.51 μm) for thermal infrared band 11. Landsat 8 has a temporal resolution of 16 days, so the satellite should capture an image of each geographical area during this date (https://earthexplorer.usgs.gov.).

Data from Landsat 8 has been extensively used to extract information on surface temperatures for both land and water. By transforming digital numbers into radiance, it is possible to determine the temperature (Hamzaa *et al.,* 2022). The temperature extraction equation, either in Kelvin or Silesian, is then used. A function called "brightness temperature" that directly extracts surface temperature has recently been added to ENVI 5.3 (Hamzaa *et al.,*2022). Based on the environmental and physical circumstances, this equation's spatial accuracy varies, being more exact in some geographical areas than others.

Due to this, appropriate statistical metrics are used to evaluate the precision of thermal models retrieved from satellites. On the other hand, regression analysis is commonly used to adjust the values of satellite pixels depending on field measurements. SST has already been discussed in several studies in the North Arabian Gulf. Some are based on thermal data from the Advanced Very High-Resolution Radiometric (AVHRR) with a spatial resolution of 4 km2 (Al-Rashidi *et al.,* 2009; Al-Fartusi *et al.,* 2023). Others make use of MODIS products with 1 km2 spatial resolution (Moradi and Kabiri, 2015; Barseem, 2014; Ghanea, 2016). In addition, assorted studies relied on field measurements to map SST over the region (Alyamani *et al.,* 2004). The study aims to use the thermal bands of Landsat 8 to estimate sea surface temperature by evaluating the accuracy of the "brightness temperature equation" using field data collected in Iraqi territorial waters in 2014 and 2022.

Research Region

In the Northwest of Arabian Gulf's, three measuring stations were selected Figure 1. The first station is located at the start of the Shatt al-Arab mouth, the second is at the entrance to marine waters, and the third station is located at the beginning of Khor Abdullah. Thus, it is distributed in the Iraqi territorial waters. These stations were chosen because of the scarcity of measurements, and if any, they are at far-apart time intervals.

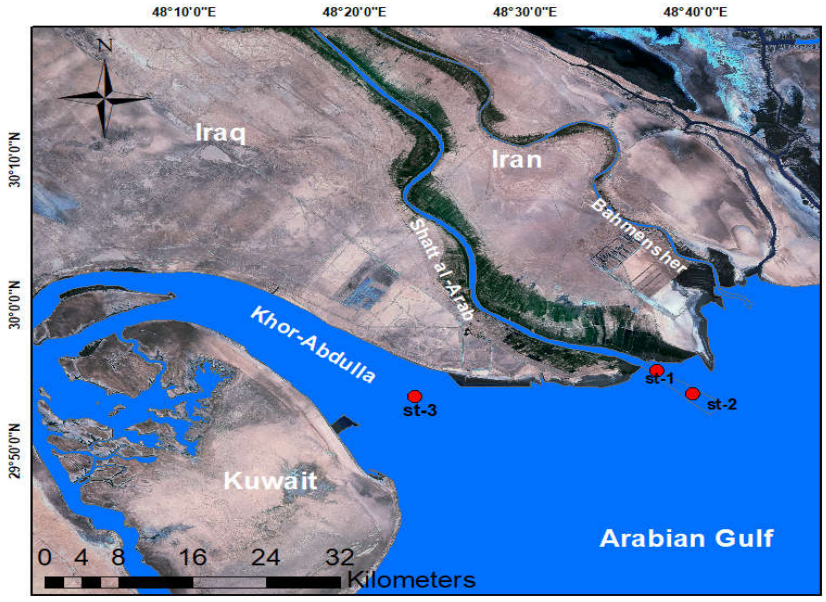

Figure 1. Study Area and Measurement Stations

Methodology:

Two types of measurements were used in this paper: field data and satellite images.

Data Description and Fieldwork:

In this study, we relied on SST-specific data that were measured at the above-mentioned measurement stations conducted during the study period of this research in 2022, in addition to data measured in 2014 by the researcher (Abdulnabi, 2016). Also, Landsat 8 satellite images were downloaded on the same day of the measurement, using the archive of Landsat 8 satellite images, from the USGS website.

Data Pre-Processing:

ENVI 5.3 software was utilized to pre-process the Landsat 8 images. Eleven bands make up the Landsat 8 image; the TIRS sensor's two thermal bands are among them Figure 2. The ENVI 5.3 software function provided under radiometric calibration tools was utilized to convert digital numbers (primary format in which data are stored) in Landsat 8's two thermal bands into brightness temperature to extract the temperature of the land's surface, "including water". The formula below is used to calculate this function (Hamzaa *et al.,* 2022).

The following literature describes the steps included in the present work:
Equation (1) is used in the first step of the submitted work to convert the satellite-based digital number (DN) into sensor spectral radiation (Lλ′).

$$L_{\lambda}' = M_L * Q_{cal} + A_L \ldots\ldots\ldots (1)$$

Where: M_L= Band-specific-multiplicative rescaling factor from the metadata.
Q_{cal} = Quantized and calibrated standard product DN value of the pixel, and A_L = Band-specific additive rescaling factor from the metadata.

In the second step, the coefficients K1 and K2 were then used to calculate the effective at-satellite temperature. Equation (2) is the conversion equation.

$$T = \frac{K2}{\ln\left(\frac{K1}{L_{\lambda'}}+1\right)} \ldots\ldots\ldots\ldots\ldots\ldots (2)$$

K1 and K2, which are found in the metadata file associated with the satellite image, are the thermal constants of TIRS bands 10 and 11. The effective at-satellite temperature is denoted by T, in kelvin (K).
Absolute zero is approximately equal to (-273.15), which had to be added to have the results in Celsius (C^o).
The thermal infrared bands ought to be transformed to brightness temperature (BT) utilizing equation (3) and metadata .

$$BT = T - 273.15 \ldots\ldots\ldots\ldots (3)$$

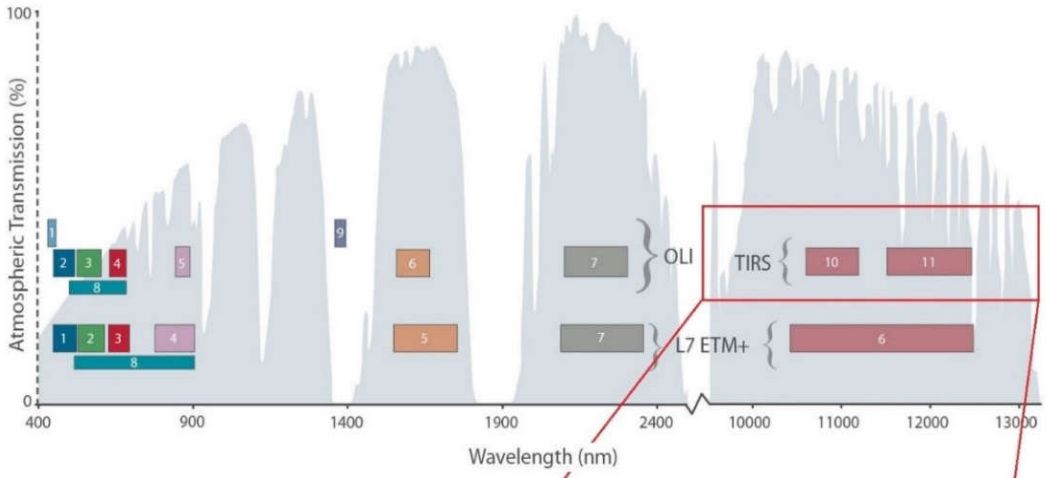

Landsat 8 Operational Land Imager (OLI) and Thermal Infrared Sensor (TIRS)	Band	Wavelength (micrometers)	Resolution (meters)
	Band 1 - Coastal aerosol	0.43 - 0.45	30
	Band 2 - Blue	0.45 - 0.51	30
	Band 3 - Green	0.53 - 0.59	30
	Band 4 - Red	0.64 - 0.67	30
	Band 5 - Near Infrared (NIR)	0.85 - 0.88	30
	Band 6 - SWIR 1	1.57 - 1.65	30
	Band 7 - SWIR 2	2.11 - 2.29	30
	Band 8 - Panchromatic	0.50 - 0.68	15
	Band 9 - Cirrus	1.36 - 1.38	30
	Band 10 - Thermal Infrared (TIRS) 1	10.60 - 11.19	100
	Band 11 - Thermal Infrared (TIRS) 2	11.50 - 12.51	100

Figure 2. The spatial resolution and atmospheric transmission range of the Landsat 8 spectral bands (https://usgs.gov/media/images/landsat-8-band-designations).

Geospatial Analysis:

Each measurement point is surrounded by a buffer covering 1 km^2 of the Landsat 8 thermal image to match the two thermal bands of the satellite with the field measurements. Values extracted from two thermal bands for every image with the field measurements were compared by counting the root mean square error and the mean absolute percentage error. Statistics show the rate of variation between the two variables in the measurement unit being used. In this analysis, MAPE was expressed in percentages, whereas RMSE was expressed in degrees. The next formulas were utilized to compute RMSE and MAPE.

$$\text{RMSE} = \pm\sqrt{\frac{1}{n}\sum_{i,j=1}(f_i - f_j)^2} \quad \text{.....(4)}$$

$$\text{MAPE} = \frac{1}{n}\sum_{i,j=1}\left|\frac{f_i - f_j}{f_i}\right| 100 \quad \text{.....(5)}$$

Where f_i is the field measurement value and f_j is the mean value of Landsat 8 thermal bands in pixels, Figure 3. Displays a summary of the methodology.

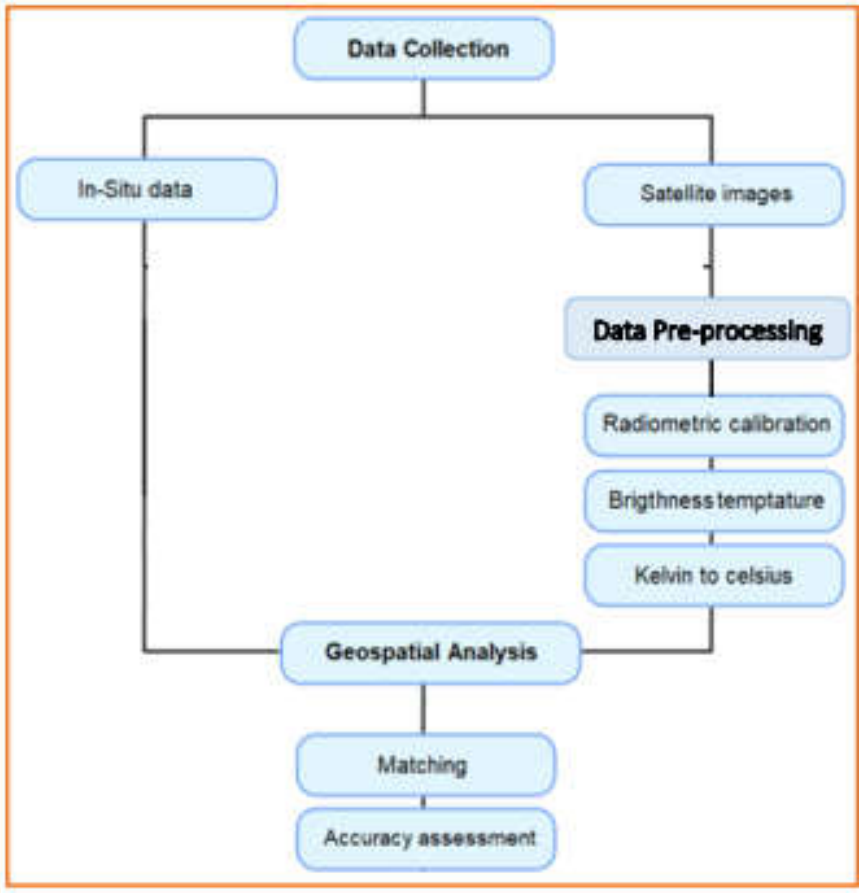

Figure 3. Flow chart of the current study's methodology

Results and Discussion:

Using measurements from field surveys and thermal images, the precision of ENVI 5.3 software's "brightness temperature" function in extracting SST for Iraqi territorial waters using two thermal bands of Landsat 8 was assessed in Figures 4a, b, and 5a,b. Based on statistical indicators like RMSE and MAPE, it was discovered that thermal band 10 of Landsat 8 was the best at extracting SST compared to band 11, northwest Arabian Gulf (Table 1), where the thermal band 10 precision was ±21.7 (1.79%) and the precision of the thermal band 11 was ±2.37 (2.49%). In 2014, with a difference ± 0.65 (0.7%). Whilst, in 2025, it was found that the precision of the thermal band 10 was ± 1.7 (2.37%) and the precision of the thermal band 11 was ±2.23 (3.13%), with a difference of ± 0.55 (0.76%).

This agrees with (Susilo *et al.,* 2019), who conducted a study along the Wangi Wanji island coast of Indonesia and discovered that the brightness temperature value produced by the spectral characteristics of band 10 is higher than that of band 11. The blackbody radiation theory-based Planck's law curves may be to blame for this.

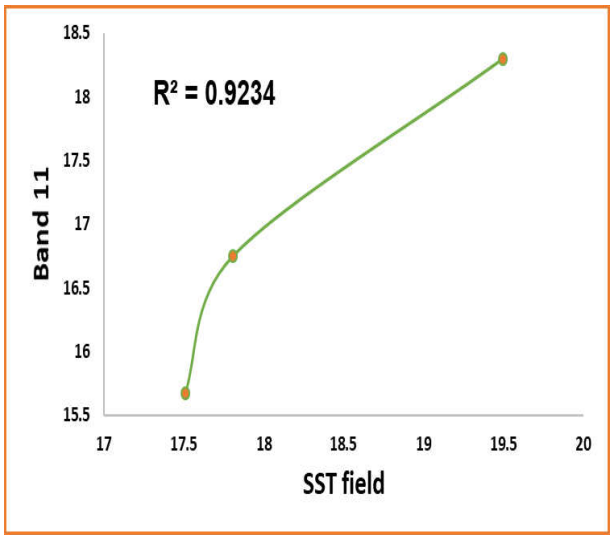

Figure 4b. The relation between thermal infrared band 11 and field data (2014).

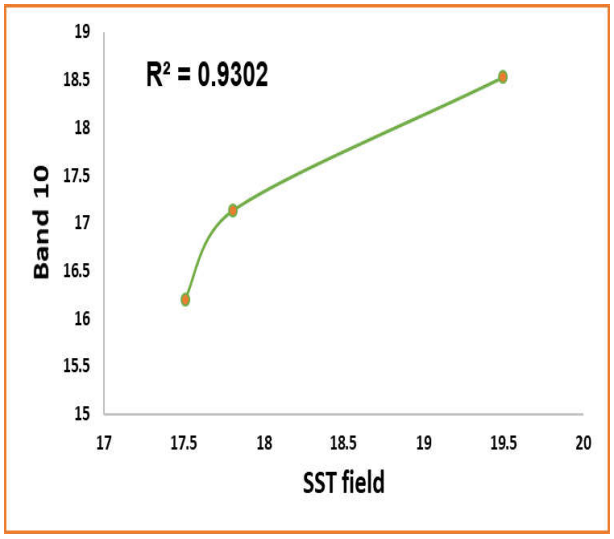

Figure 4a. The relation between thermal infrared band 10 and field data (2014).

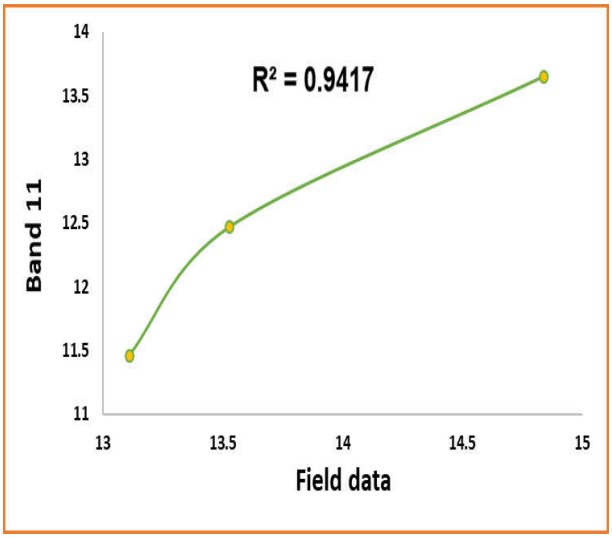

Figure 5b. The relation between thermal infrared band 11 and field data (2022)

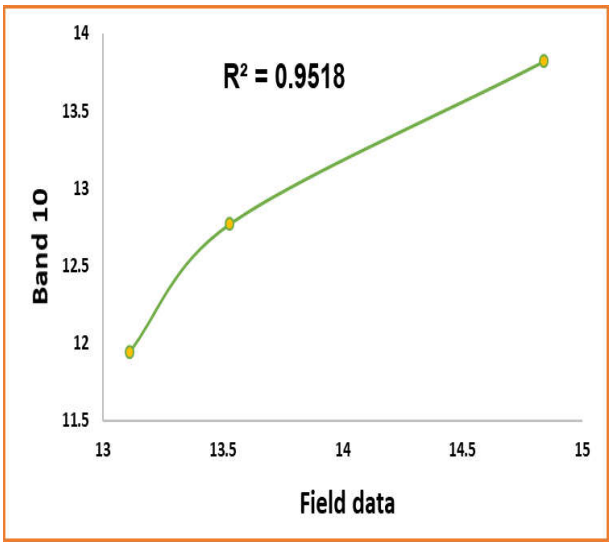

Figure 5a. The relation between thermal infrared band 10 and field data (2022).

Table 1. *RMSE, MAPE, and R^2 scores*

	2014			2022		
	RMSE	MAPE %	R^2	RMSE	MAPE %	R^2
Thermal band 10	1.72	1.79	0.93	1.7	2.37	0.95
Thermal band 11	2.37	2.49	0.92	2.25	3.13	0.94

Conclusion:

In this study, two years of field measurements were used to assess the precision of Landsat 8 thermal ranges (2014 and 2022). According to the results, it is advised that Landsat 8's thermal band 10 be utilized to measure sea surface temperatures in the northwest Arabian Gulf when utilizing the function of brightness temperature.

Recommendations:

A. Conducting more research and studies to develop a new model with greater precision for monitoring sea surface temperature in this region.
B. Using more than one measuring station distributed throughout the Arabian Gulf's northwest region to create a thermal map of the region.

Acknowledgments

We would like to express our gratitude to the scientific team of the Marine Physics Department at the University of Basrah Marine Science Center for their help with our work.

References:

Abdulnabi Z. A. , 2016. Assessment of some toxic elements levels in Iraqi marine water, Mesopotamian Journal of Marine Sciences, 31 (1): 85–94.

Ahn Y. H. , Shanmugam P., Lee, J. H. , and Kang, Y. Q. 2006. Application of satellite infrared data for mapping of thermal plume contamination in the coastal ecosystem of Korea, Marine Environment of Research, 61, (2) : 186–201. DOI: 10.1016/j.marenvres.2005.09.001.

Al-Fartusi, A. J., Malik, M. I. and Abduljabbar, H. M. , 2023. Utilizing Spectral Indices to Estimate Total Dissolved Solids in Water Body Northwest Arabian Gulf, Ilmu Kelautan: Indones. Journal of Marine Sciences, 28 (3) : 217–224 . DOI: 10.14710/ik.ijms.28.3.217-224

Al-Rashidi, T. B., El-Gamily, H. I., Amos, C. L., and Rakha, K. A. 2009. Sea surface temperature trends in Kuwait Bay, Arabian Gulf. Natural Hazards, 50 (1):73–82. DOI: 10.1007/s11069-008-9320-9.

Alyamani, F., Bishop, J., Ramadhan, E., Al-Husaini, M., and Al-Ghadban, A. 2004. Oceanographic Atlas of Kuwait's Waters, 1st ed., Kuwait Institute for Scientific Research.

Barseem, M. S., El-Sayed, A. N. and Youssef, A. M. 2014. Impact of geologic setting on the groundwater occurrence in wadis El Sanab, Hashem, and Khrega using geoelectrical methods – north-western coast, Egypt. Arabian Journal of Geosciences, 7: 5127–5139. DOI: 10.1007/s12517-013-1129-5.

Corlett, G. K. , Barton, I. J. , Donlon, C. J. , Edwards, M. C. , Good, S. A. , Horrocks, L. A. , Llewellyn-Jones, D. T. , Merchant, C. J. , Minnett, P. J. , and Nightingale, T. J. 2006. The accuracy of SST retrievals from AATSR: An initial assessment through geophysical validation against in situ radiometers, buoys, and other SST data sets. Advances Space Research, 37(4):764–769.https://doi.org/10.1016/j.asr.2005.09.037.

Dash, P., Ignatov, A. , Kihai, Y., and Sapper, J. 2010. The SST quality monitor (SQUAM). Journal of Atmospheric and Oceanic Technology, 27(11): 1899–1917. https://doi.org/10.1175/2010JTECHO756.1.

Elhakeem, A., Elshorbagy, W., and Bleninger, T., 2015. Long-term hydrodynamic modelling of the Arabian Gulf. Marine Pollution Bulletin, 94 (1–2):19–36. DOI:10.1016/j.marpolbul.2015.03.020.

Ghanea, M. , Moradi, M., Kabiri, K., and Mehdinia, A., 2016. Investigation and validation of MODIS SST in the northern Persian Gulf, Advances Space Research, 57 (1): 127–136. DOI: 10.1016/j.asr.2015.10.040.

Hamzaa, M. T., Malik, M. I., and Al-Shammary, S. H. , 2022. Study of Desertification in the East of Iraq in (2013–2020) by Supervised Maximum Likelihood. AIP Conference Proceedings, 2437 (1): p. 020025. https://doi.org/10.1063/5.0094006

Moradi, M. and Kabiri, K., 2015. Spatio-temporal variability of SST and Chlorophyll-a from MODIS data in the Persian Gulf. Marine Pollution Bulletin, 98 (1–2): 14–25. DOI: 10.1016/j.marpolbul.2015.07.018.

Nesterov, O., Temimi, M. , Fonseca, R., Nelli, N. R. , Addad, Y. , Bosc, E. and Abida, R., 2021. Validation and statistical analysis of the Group for High-Resolution Sea Surface Temperature data in the Arabian Gulf. Oceanologia, 63(4): 497–515. https://doi.org/10.1016/j.oceano.2021.07.001

Park, K. A., Chung, J. Y., and Kim, V. 2004. Sea surface temperature fronts in the East (Japan) Sea and temporal variation. Geophysical Research Letters, 31(7). https://doi.org/10.1029/2004GL019424.

Reynolds, R. M. 1993. Physical oceanography of the Gulf, Strait of Hormuz, and the Gulf of Oman - Results from the Mt Mitchell expedition. Marine Pollution. Bulletin., 27: 35–59. DOI: 10.1016/0025-326X(93)90007-7.

Susilo, E., Hannity, R. and Wijeya, A. 2019. Retrieving coastal sea surface temperature from Landsat-8 TIRS for Wangi-Wangi Island, Wakatobi, Southeast Sulawesi, Indonesia. International Journal of Remote Sensing and Earth Science, 16 (1) : 13–22. https://doi.org/10.30536/ijreses.v16i1.13833.

Syariz, M. A., Jaelani, L. M., Subehi, L., Pamungkas, A., Koenhardono, E. S. and Sulisetyono, A. , 2015. Retrieval of sea surface temperature over Poteran Island water of Indonesia with Landsat 8 TIRS image: A preliminary algorithm. The International Archives of the Photogrammetry, Remote Sensing and Spatial Information Sciences, 40, 87-90. DOI: 10.5194/isprsarchives-XL-2-W4-87-2015.

Ullman, D. S. and Cornillon, P. C. 2000. Evaluation of front detection methods for satellite-derived SST data using in situ observations. Journal of Atmospheric and Oceanic Technology,17(12):1667–1675.

USGS, Earth Explorer, 2021. [Online]. Available: https://earthexplorer.usgs.gov. USGS, "Landsat 8 band designations." [Online]. Available: https://usgs.gov/media/images/landsat-8-band-designations.

Wloczyk, C., Richter, R., Borg, E. and Neubert, W. 2006. Sea and lake surface temperature retrieval from Landsat thermal data in Northern Germany. International Journal of Remote Sensing, 27 (12) : 2489–2502 DOI: 10.1080/01431160500300206.

Xue, P. and Eltahir, E. A. B. 2015. Estimation of the heat and water budgets of the Persian (Arabian) Gulf using a regional climate model. Journal of Climate, 28: 5041–5062. DOI: 10.1175/JCLI-D-14-00189.1.